Opto-Electronic Advances

Original Article

2020, Vol. 3, No. 7

DOI: 10.29026/oea.2020.190033

10-GHz broadband optical frequency comb generation at 1550/1310 nm

Junyuan Han[1,2,4†], Yali Huang[3†], Jiliang Wu[1,2], Zhenrui Li[3], Yuede Yang[1,2], Jinlong Xiao[1,2], Daming Zhang[3], Guanshi Qin[3*] and Yongzhen Huang[1,2*]

The generation of high-repetition rate (f_{rep} ≥ 10 GHz) ultra-broadband optical frequency combs (OFCs) at 1550 nm and 1310 nm is investigated by seeding two types of highly nonlinear fibers (HNLFs) with 10 GHz picosecond pulses at the pump wavelength of 1550 nm. When pumped near the zero dispersion wavelength (ZDW) in the normal dispersion region of a HNLF, 10 GHz flat-topped OFC with 43 nm bandwidth within 5 dB power variation is generated by self-phase modulation (SPM)-based OFC spectral broadening at 26.5 dBm pump power, and 291 fs pulse trains with 10 GHz repetition rate are obtained at 18 dBm pump power without complicated pulse shaping methods. Furthermore, when pumped in the abnormal dispersion region of a HNLF, OFCs with dispersive waves around 1310 nm are studied using a common HNLF and fluorotellurite fibers, which maintain the good coherence of the pump light at 1550 nm. At the same time, sufficient tunability of the generated dispersive waves is achieved when tuning the pump power or ZDW.

Keywords: optical comb; electro-optic devices; ultrafast optics; optical pulses; nonlinear optics

Han J Y, Huang Y L, Wu J L, Li Z R, Yang Y D et al. 10-GHz broadband optical frequency comb generation at 1550/1310 nm. *Opto-Electron Adv* **3**, 190033 (2020).

Introduction

Passively mode-locked laser frequency combs with typical sub-GHz repetition frequency and sub-100-fs optical pulses have revolutionized optical frequency metrology and precision timekeeping by providing an equidistant set of absolute reference lines that span in excess of an octave[1]. For applications such as calibration of astronomical spectrographs[2,3], optical arbitrary waveform generation[4,5], microwave signal processing[6], and coherent communications[7], higher repetition frequency comb (f_{rep} ≥ 10 GHz) has become a more effective implement. However, the passively mode-locked laser with higher repetition rate requires a shorter physical cavity in the optical domain, which needs complex design and operation[8]. Consequently, the tolerance required to control such a cavity length decreases to a scale that is difficult to be physically realized. In order to increase the line spacing of passively mode-locked laser frequency combs, Fabry-Pérot cavities are used to act as periodic, high resolution spectral filters, which require servo control and increase the complexity of the system[2].

Actively mode-locked laser[9,10] and electro-optic modulation[11–13] can directly generate optical frequency combs (OFCs) at a higher repetition rate, whose repetition rate is no longer limited by the cavity length but determined by the modulation frequency. However, the achievable optical bandwidth generated by the external modulation is limited by the electro-optic modulation efficiency and the ability of the modulator to carry radio frequency power[9,12,14]. Meanwhile, pulses with higher repetition rate

[1]State Key Laboratory of Integrated Optoelectronics, Institute of Semiconductors, Chinese Academy of Sciences, Beijing 100083, China; [2]Center of Materials Science and Opto-Electronic Engineering, University of Chinese Academy of Sciences, Beijing 100049, China; [3]State Key Laboratory of Integrated Optoelectronics, College of Electronic Science & Engineering, Jilin University, Changchun 130012, China; [4]National Key Laboratory of Science and Technology on Electronic Test and Measurement, the 41st Research Institute, China Electronics Technology Group Corporation, Qingdao 266555, China.

[†]These authors contributed equally to this work.

*Correspondence: G S Qin, E-mail: qings@jlu.edu.cn; Y Z Huang, E-mail: yzhuang@semi.ac.cn

Received: 1 September 2019; Accepted: 20 January 2020; Published: 22 July 2020

will result in lower peak power at a limited average optical power, which prevents the generation of broadband flat OFC[15]. In order to overcome the limitations above, HNLF was applied to broaden high-repetition rate OFC. Nonlinear generation of ultra-flat broadened spectrum was achieved with adaptive pulse shaping[4,16], and 10 GHz flat OFCs was obtained using a wavelength selective element after the HNLF[17]. By applying complicated stress to HNLF, a flat frequency comb can be generated using a parametric gain[18–20]. Recently, resonant electro-optic frequency comb has been extensively studied for their high electro-optic conversion efficiency and the ability to easily generate broadband OFC[21,22]. Although the optical bandwidth of 80 nm has been achieved, the spectral flatness needs to be further improved.

In this paper, we study the broadband OFC generation with a repetition rate of 10 GHz covering 1550 nm and 1310 nm by using two types of HNLFs with different dispersion at the pump wavelength of 1550 nm. Firstly, we theoretically and experimentally confirm that picosecond pulses with high repetition rates can generate broadband flat OFC and ultrashort pulses at 1550 nm by SPM effect at relatively low pump power without using any optical filter components for controlling. Then, by adjusting the power of pump light and the ZDW of HNLFs, we generate dispersive waves around 1310 nm with sufficient tunability and good coherence with the pump wavelength of 1550 nm.

Results and discussion

Generation of OFCs and ultra-short pulses

The frequency interval of the optical comb depends on the repetition rate of the seed pulse (Fig. 1(a)), which is locked to the 10 GHz microwave source. An optical spectrum analyzer (OSA) is used to record the generated OFC. The frequency resolved optical gating (FROG) technology which uses the optical nonlinear process of second harmonic generation is employed to resolve ultra-short optical pulses[23]. Initially, a 2.3-ps-wide-Gaussian, almost-chirp-free pulse is obtained from a mode-locked laser (Pritel ultrafast optical clock), as shown in Fig. 1(b).

For achieving spectral broadening, the 2.3-ps pulse is amplified by an Erbium-Ytterbium co-doping fiber amplifier (EYDFA) and fed into a 500 m HNLF with the group velocity dispersion (GVD) of ~0.293 ps^2/km (see supplementary material), nonlinear coefficient of ~10.8 (W·km)$^{-1}$ and fiber attenuation of ~0.2 dB/km at 1550 nm, which is used to induce SPM effect for generating broadband OFCs. Schematic diagrams of the experimental setup for OFC and ultra-short pulse is shown in the selected section of Fig. S3(b) in supplementary material. Optical spectra after propagation through the 500 m HNLF are plotted in Fig. 2(a) at the pump powers of 15 dBm, 17 dBm, 19 dBm and 20 dBm. Compared with the spectrum shown in Fig. 1(a), the spectral flatness is improved by SPM effect in the HNLF. For a qualitative study, we solve the following generalized nonlinear Schrödinger equation using the split-step Fourier method[24–26],

$$\frac{\partial A}{\partial z}+\frac{\alpha}{2}A+\sum_{k\geq 2}\frac{\mathrm{i}^{k-1}\beta_k}{k!}\frac{\partial^k A}{\partial t^k}= \mathrm{i}\gamma\left(1+\frac{\mathrm{i}}{\omega_0}\frac{\partial}{\partial t}\right)\left[A(z,t)\times\int_{-\infty}^{\infty}R(t')\left|A(z,t-t')\right|^2\mathrm{d}t'\right] \quad , (1)$$

where A is the envelope of the pulse electric field and ω_0 is the center frequency of the input pulse. The fiber loss, dispersion, and nonlinear coefficient are α, β, and γ, respectively, and $R(t)$ is the response function of the silica fiber. The 4th-order Runge-Kutta algorithms are used in the simulation, and as high as 4th order dispersion was taken into account in the calculation. The numerical results as shown in Fig. 2(b) are in agreement very well with the experimental results. The slightly difference in pump power between Figs. 2(a–b) are owing to the distortion of

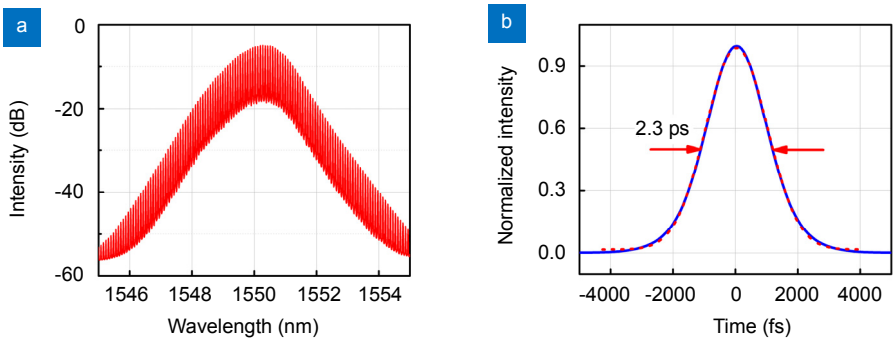

Fig. 1 | The 10 GHz OFC and a 2.3-ps pulse generated from a mode-locked laser with (a) OFC spectrum, and (b) reconstructed temporal pulse profile (blue solid curve) and Gaussian fitting curve (red dotted curve).

the optical pulse caused by the dispersion of erbium-doped fiber to amplify the optical pulse in the experiment. The corresponding optical time domain pulse obtained after pumping 500 m HNLF with different power is shown in Fig. S2 in Supplementary Information.

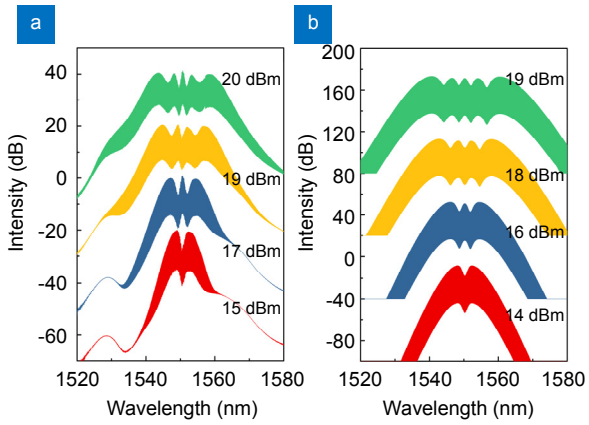

Fig. 2 | Optical spectra after propagation in 500 m HNLF. (**a**) The experimental results when the input optical power into the HNLF is 15 dBm, 17 dBm, 19 dBm, 20 dBm, respectively. (**b**) The simulation results when the input optical power is 14 dBm, 16 dBm, 18 dBm, 19 dBm, respectively.

To show the quality of the generated OFC, the whole broadened frequency comb at 20 dBm pump power is detected by a 50 GHz photodiode (PD) with a responsivity of 0.7 A/W. The beat note microwave signal is analyzed by an electrical spectrum analyzer (ESA), as shown in Fig. 3(a). The side mode suppression ratio (SMSR) of the 10 GHz beat signal is measured to be more than 75 dB with a resolution bandwidth (RBW) of 200 kHz and video bandwidth (VBW) of 50 kHz. Owing to the positive chirp introduced by SPM, the pulse compression can be achieved through a dispersive single mode fiber (SMF) with chirp compensation. Figure 3(b) shows the reconstructed pulse profile obtained through FROG and a pulse with a full width at half maximum (FWHM) of 291 fs is obtained through a 4 m SMF without complicated optical component such as pulse shaper[4]. Pulse compression is accompanied by strong spectral broadening. The ability to obtain microwave signal with high SMSR and achieve pulse compression shows that the generated OFC has a very good coherence. This ultra-short pulse train with high peak power is very useful for the generation of octave-spanning supercontinuum (SC) spectrum[15], and the pulse will be used in our experiments below.

Generation of broadband OFCs using silica HNLFs

To further investigate the spectral broadening, the pump power is increased to 26.5 dBm. Schematic diagram of the experimental setup for the generation of broadband OFCs is shown in Fig. S3(a) in Supplementary Information. The 10 GHz flat-topped OFC with 43 nm bandwidth and more than 500 spectral lines within 5 dB power variation is generated without any optical filter, as shown in Fig. 4(a). The strong SPM effect occurs in the HNLF resulting in the generation of broadband OFC. Different from passively mode-locked laser, the repetition rate of the generated OFC is no longer determined by the cavity length but by the frequency of the external microwave signal applied to the modulator which can be tuned by simply changing the modulation frequency. Hence, the generated frequency comb is broadly tunable in the repetition rate. Furthermore, the 18.5 GHz flat OFC is generated at 25.5 dBm pump power, as shown in Fig. 4(b). If the microwave source with higher output frequency and the modulator with larger modulation bandwidth are used, the frequency comb with higher repetition rate can be generated.

Next, 1310 nm broadband OFC is generated using the 2.3 ps pulse at the center wavelength of 1550 nm with higher power. Schematic diagrams of the experimental

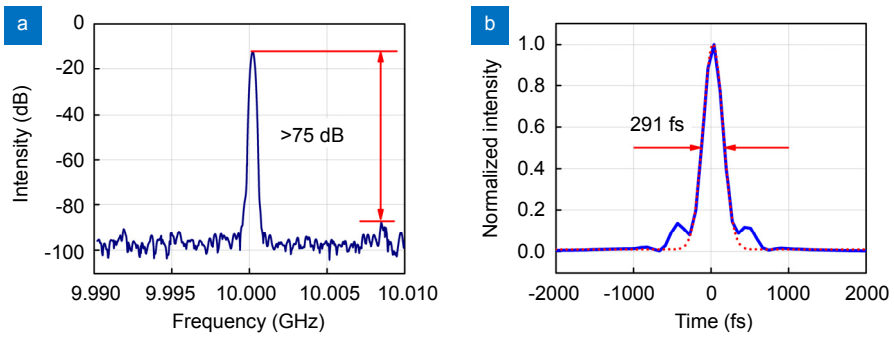

Fig. 3 | (**a**) RF spectrum from the broadened frequency comb at 20 dBm pump power (RBW=200 kHz and VBW=50 kHz). (**b**) Reconstructed temporal pulse profile with a FWHM duration of 291 fs after transmitting a 4 m SMF at 20 dBm pump power (blue solid curve) and Gaussian fitting curve (red dotted curve).

setup for the generation of broadband OFC is shown in Fig. S3(a) in Supplementary Information. It is important to pump at anomalous dispersion region of the HNLF to achieve the broadband SC spectrum and to support soliton propagation[27]. A 500 m HNLF is used with the dispersion of ~ -0.496 ps^2/km, the nonlinear coefficient of ~10 (W·km)$^{-1}$ and the fiber attenuation of ~0.762 dB/km at 1550 nm. As shown in Fig. 5(a), the dispersive wave generated at 1310 nm providing local spectral enhancement occurs in the normal dispersion regime where phase matching is achieved between the fundamental soliton and a small-amplitude linear wave of different frequency[24]. As the pump power increases from 31 dBm to 33 dBm, the center wavelength of the dispersive wave shifts from 1351 nm to 1305 nm, where the tunable range of the dispersive wave is greater than 40 nm. However, the SC generation requires a long fiber at low pumping power and the coherence of the SC is largely degraded due to the nature of modulation instability. Although the coherence degradation normally occurs due to the amplification of the noise in the pulse by the modulation instability, the dispersive wave can also maintain the good coherence of the pump light[28]. A 1550/1310 nm array waveguide grating is used to filter out 1550 nm pump light, and then microwave signal is generated by a 50 GHz PD using the pulse around 1310 nm. The microwave signal measured by an ESA is shown in Fig. 5(b). The SMSR of the 10 GHz beat note is measured to be 26 dB at 32 dBm pump power, which confirms certain coherence of the dispersion wave.

Generation of broadband OFCs using fluorotellurite fibers

In order to reduce the effect of the modulation instability on the coherence of the optical frequency comb, we fabricated and used fluorotellurite fibers with a high nonlinear coefficient and a short length. Very recently, fluorotellurite fibers with a high nonlinear coefficient, good water resistance and high transition temperature, became the promising nonlinear medium for high power mid-infrared SC generation (f_{rep} ≤100 MHz) for their rich spectral broadening mechanism such as self-phase modulation, soliton fission, soliton self-frequency shift, and dispersive wave generation[29,30]. In the experiment, fluorotellurite fibers were fabricated by rod-in-tube method, and the compositions with a large refractive index difference of the core and the cladding layers are 70TeO_2-20BaF_2-10Y_2O_3 (TBY) and 33AlF_3-11MgF_2-17CaF_2-8SrF_2-9BaF_2-12YF_3-10TeO_2 (AMCSBYT)[31], respectively. Insets in Fig. 6 show the cross sections of the fibers with the core diameters of 3.7 μm, 3.3 μm and 3.1

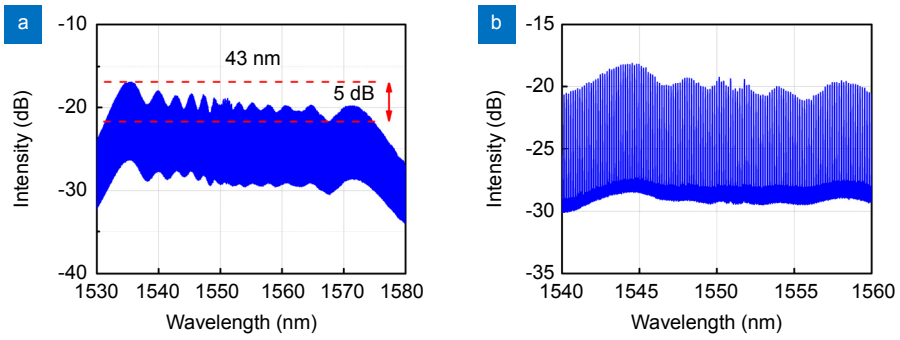

Fig. 4 | Optical spectra of the generated flat-topped OFC. (**a**) The 10 GHz repetition rate at 26.5 dBm pump power. (**b**) The 18.5 GHz repetition rate at 25.5 dBm pump power.

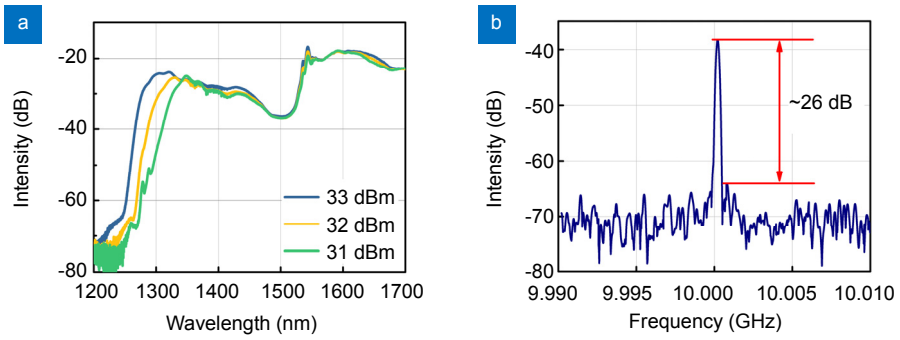

Fig. 5 | (**a**) Experimental supercontinuum spectra designed to produce a dispersive wave centered around 1310 nm. (**b**) RF spectra from the generated 1310 nm dispersion wave at 32 dBm pump power (RBW=200 kHz and VBW=50 kHz).

μm. Corresponding dispersion curves are shown in Fig. 6. The first ZDWs, 1452 nm, 1409 nm and 1358 nm, are all located at the blue side of the pump wavelength, ~1550 nm, at anomalous dispersion region of the fibers, which is the requirement for dispersive waves generation[24]. The fiber loss at 1560 nm is about 2 dB/m using a cutback method. The nonlinear refractive index of TBY glasses is as high as 3.5×10^{-19} m^2/W, and the corresponding nonlinear coefficients of the three optical fibers were evaluated to be 220, 257, 303 $(W\cdot km)^{-1}$, respectively, which are much higher than those of silica HNLFs.

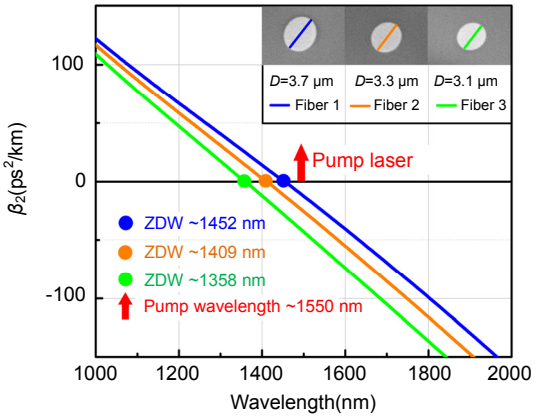

Fig. 6 | The calculated dispersions of the fibers with different sizes. Insets, scanning electron microscope images of the fibers with the diameters of 3.7 μm, 3.3 μm and 3.1 μm, respectively.

To clarify the potential of the designed fluorotellurite fibers for broadband optical frequency comb generation at the pump wavelength of 1550 nm with 10 GHz pulses, we perform the following experiments. Schematic diagram of the experimental setup for the generation of broadband OFC is shown in Fig. S3(b) in supplementary information. The pump laser is the ultrashort pulses with a pulse width less than 300 fs and the repetition rate of 10 GHz which we have generated from 2.3 ps pulses as shown in Fig. 3(b). The pumped laser is amplified and coupled into the nonlinear medium by a couple of aspheric lenses and the output broadening signals are monitored by an OSA and an ESA. The fiber length of the fluorotellurite fibers we used is 40 cm, which is not so long to deteriorate coherence. The generated SC spectra from the fluorotellurite fiber with the ZDW of 1452 nm are shown in Fig. 7(a), with average launched power of the high-repetition rate pump laser from 2.85 W to 5.56 W after pulse compression and power amplification. The pulse peak power is from 185 W to 361 W, when the repetition rate of the laser is 10 GHz and coupling efficiency is about 52%. At the same time, due to the dispersion of the high-power fiber amplifier, the pulse of 300 fs is broadened to about 800 fs. The GVD is about -40 ps^2/km at the pump wavelength, located at the anomalous dispersion region of the fiber. For a 40 cm length fiber, the first soliton fission occurs when the pulse peak power reaches 260 W, and so does the dispersive wave. With a further increasing of the average pump power, it is clearly observed that the output SC spectrum becomes broader for the soliton self-frequency shift at the red side owing to the Raman effect and the dispersive wave emission at the blue side[24]. When the pulse peak power reaches 361 W, the wavelength of dispersive wave is located at around 1310 nm with an ideal intensity. The phenomena of dispersive wave emission at the blue side in the fiber with such dispersion profiles could be explained and conform to that in the preceding paragraphs.

The influence of different ZDWs on dispersion waves is studied at fixed average pump power at 5.96 W, as shown in Fig. 7(b). At short wave, the wavelength of dispersive waves emit in the normal GVD regime depends mainly on power and the first ZDW. The central wavelengths of dispersive waves are 1155 nm, 1250 nm and 1310 nm, corresponding to ZDWs from short to long wave, respectively. The measured output powers of the SC

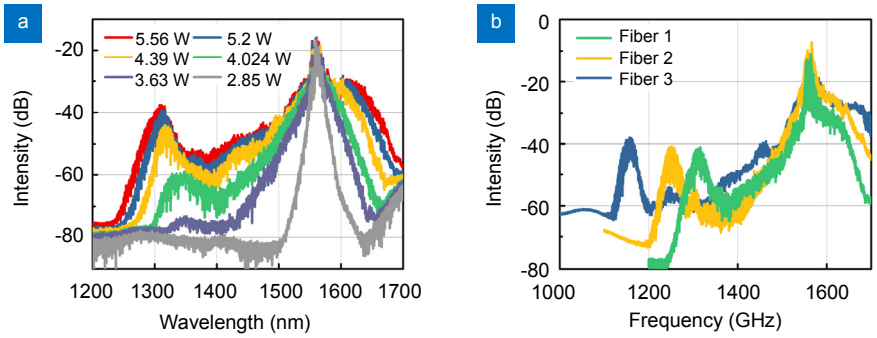

Fig. 7 | (**a**) Optical spectra with a dispersive wave centered around 1310 nm from a fluorotellurite fiber under different launched powers of the femtosecond laser. (**b**) Optical spectra with tunable dispersive waves ranging from 1150 nm to 1310 nm from fluorotellurite fibers 1, 2, 3 with ZDWs at 1358 nm, 1409 nm and 1452 nm, respectively.

spectra are about 1.37 W, 1.9 W and 2.38 W for an average pump power of 5.96 W. The maximum broadening of the spectrum is limited by the pulse width and average power of the pump light, which could be optimized in the future. Meanwhile, our fibers remain intact with no damage during the whole high-power experiment. The results have shown that the 1100–1400 nm tunable dispersion waves with the comb spacing of 10 GHz could be obtained in fluorotellurite fibers at the pump wavelength of 1550 nm.

In addition, the generalized nonlinear Schrödinger equation (1) is solved numerically to investigate the spectral broadening mechanism. High order (as high as 8th) dispersion was taken into account. The Raman response function coefficients in Eq. (2) are f_R = 0.064, τ_1 = 7.2 fs and τ_2 = 59.3 fs, respectively.

$$R(t)=(1-f_R)\delta(t)+f_R\frac{\tau_1^2+\tau_2^2}{\tau_1\tau_2^2}\exp\left(-\frac{t}{\tau_2}\right)\sin\left(\frac{t}{\tau_2}\right)\Theta(t). \quad (2)$$

Light source parameters are set as follows: operating wavelength of 1550 nm, pulse width of 800 fs, repetition rate of 10 GHz, and pulse peak power of 387 W. Figure 8(a) shows the comparison between the simulated and measured SC spectra from the fluorotellurite fiber with the ZDW of 1452 nm, and the results are basically consistent, especially at the wavelength of the dispersion wave. The result of the simulation (red curve) is the spectrum corresponding to the single pulse. Since the pump pulse used to generate the SC has a sub-picosecond duration, modulation instability should still be the dominant dynamics in the spectrum broadening, which is very sensitive to the variation of pump power and noise. Thus, the deep notches shown by the red curve should have been washed out when the SC spectra obtained in different pulse shots are averaged in the OSA. And the differences between the width of the spectra and the wavelength of the dispersive waves may come from the pulse settings in simulation for the pulse we used could not be fitted by Gaussian function in practice. In order to verify the coherence of the generated dispersive wave in the fluorotellurite fiber, the dispersion wave is detected by a 50 GHz PD again and the beat note signal with 70 dB SMSR is characterized by an ESA, as shown in Fig. 8(b). When comparing Fig. 5(b) with 8(b), the dispersive wave generated in the fluorotellurite fiber can maintain better coherence, because the amplification of the noise caused by modulation instability in the anomalous dispersion regime is greatly reduced using a short fluorotellurite fiber. The results show that fluorotellurite fibers could be used to generate coherent dispersive wave at the wavelength of 1310 nm with the repetition rate of 10 GHz.

Conclusions

In conclusion, we have generated broadband OFCs with good coherence based on a 10 GHz picosecond pulse. The key significance of the proposed approach is that the strong SPM effect and dispersion wave could generate broadband OFCs in 1550/1310 nm. In the normal dispersion region of a HNLF, 10 GHz flat-topped OFCs with 43 nm bandwidth within 5 dB power variation are generated by SPM without any optical filter. At the same time, we obtain microwave signal with 75 dB SMSR and achieve 291 fs ultra-narrow pulse. Experimental results are well consistent with the simulated spectra using generalized nonlinear Schrödinger equation. In the abnormal dispersion region of the HNLF, the dispersive waves around 1310 nm are generated with tunability range more than 40 nm and the corresponding RF beating wave with a SMSR of 26 dB. At the same time, the highly coherent dispersive waves at the wavelength from 1100 to 1400 nm with a 70 dB SMSR for beating wave have been generated in the fluorotellurite fibers with different ZDWs. We expect that the generated comb lines can serve as the wavelength-division multiplexing source for multiple wavelength channels in optical communication network.

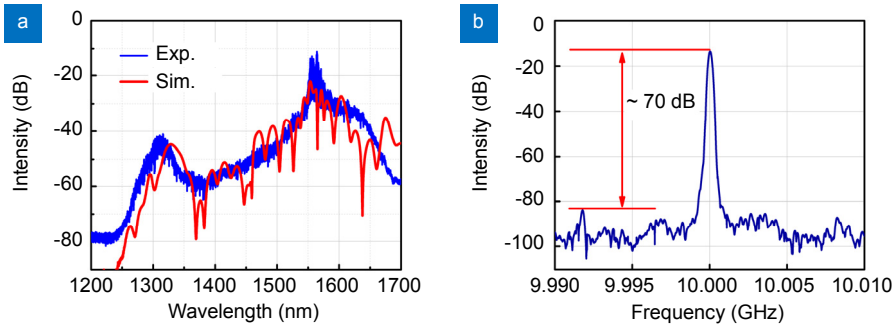

Fig. 8 | (**a**) The simulated and measured SC from the fluorotellurite fiber with the ZDW of 1452 nm and the peak pump power of 387 W. (**b**) RF spectrum from the generated 1310 nm dispersion wave in the fluorotellurite fiber (RBW=200 kHz and VBW=50 kHz).

References

1. Jones D J, Diddams S A, Ranka J K, Stentz A, Windeler R S et al. Carrier-envelope phase control of femtosecond mode-locked lasers and direct optical frequency synthesis. *Science* **288**, 635–639 (2000).
2. Quinlan F, Ycas G, Osterman S, Diddams S A. A 12.5 GHz-spaced optical frequency comb spanning> 400 nm for near-infrared astronomical spectrograph calibration. *Rev Sci Instrum* **81**, 063105 (2010).
3. Wilken T, Curto G L, Probst R A, Steinmetz T, Manescau A et al. A spectrograph for exoplanet observations calibrated at the centimetre-per-second level. *Nature* **485**, 611–614 (2012).
4. Jiang Z, Huang C B, Leaird D E, Weiner A M. Optical arbitrary waveform processing of more than 100 spectral comb lines. *Nat Photonics* **1**, 463–467 (2007).
5. Cundiff S T, Weiner A M. Optical arbitrary waveform generation. *Nat Photonics* **4**, 760–766 (2010).
6. Hamidi E, Leaird D E, Weiner A M. Tunable programmable microwave photonic filters based on an optical frequency comb. *IEEE Trans Microw Theory Tech* **58**, 3269–3278 (2010).
7. Hu H, Da Ros F, Pu M H, Ye F H, Ingerslev K et al. Single-source chip-based frequency comb enabling extreme parallel data transmission. *Nat Photonics* **12**, 469–473 (2018).
8. Bartels A, Heinecke D, Diddams S A. 10-GHz self-referenced optical frequency comb. *Science* **326**, 681 (2009).
9. Yoshida M, Yoshida K, Kasai K, Nakazawa M. 1.55 μm hydrogen cyanide optical frequency-stabilized and 10 GHz repetition-rate-stabilized mode-locked fiber laser. *Opt Express* **24**, 24287–24296 (2016).
10. Nakazawa M, Kasai K, Yoshida M. C_2H_2 absolutely optical frequency-stabilized and 40 GHz repetition-rate-stabilized, regeneratively mode-locked picosecond erbium fiber laser at 1.53 μm. *Opt Lett* **33**, 2641–2643 (2008).
11. Torres-Company V, Weiner A M. Optical frequency comb technology for ultra-broadband radio-frequency photonics. *Laser Photonics Rev* **8**, 368–393 (2014).
12. Dou Y J, Zhang H M, Yao M Y. Generation of flat optical-frequency comb using cascaded intensity and phase modulators. *IEEE Photonics Technol Lett* **24**, 727–729 (2012).
13. Wu R, Supradeepa V R, Long C M, Leaird D E, Weiner A M. Generation of very flat optical frequency combs from continuous-wave lasers using cascaded intensity and phase modulators driven by tailored radio frequency waveforms. *Opt Lett* **35**, 3234–3236 (2010).
14. Metcalf A J, Torres-Company V, Leaird D E, Weiner A M. High-power broadly tunable electrooptic frequency comb generator. *IEEE J Sel Top Quant Electron* **19**, 3500306 (2013).
15. Ishizawa A, Nishikawa T, Mizutori A, Takara H, Aozasa S et al. Octave-spanning frequency comb generated by 250 fs pulse train emitted from 25 GHz externally phase-modulated laser diode for carrier-envelope-offset-locking. *Electron Lett* **46**, 1343–1344 (2010).
16. Yang X, Richardson D J, Petropoulos P. Nonlinear generation of ultra-flat broadened spectrum based on adaptive pulse shaping. *J Lightwave Technol* **30**, 1971–1977 (2012).
17. Yang T, Dong J J, Liao S S, Huang D X, Zhang X L. Comparison analysis of optical frequency comb generation with nonlinear effects in highly nonlinear fibers. *Opt Express* **21**, 8508–8520 (2013).
18. Myslivets E, Alic N, Radic S. High resolution measurement of arbitrary-dispersion fibers: dispersion map reconstruction techniques. *J Lightwave Technol* **28**, 3478–3487 (2010).
19. Myslivets E, Kuo B P P, Alic N, Radic S. Generation of wideband frequency combs by continuous-wave seeding of multistage mixers with synthesized dispersion. *Opt Express* **20**, 3331–3344 (2012).
20. Ataie V, Temprana E, Liu L, Myslivets E, Kuo B P P et al. Ultra-high count coherent WDM channels transmission using optical parametric comb-based frequency synthesizer. *J Lightwave Technol* **33**, 694–699 (2015).
21. Rueda A, Sedlmeir F, Kumari M, Leuchs G, Schwefel H G L. Resonant electro-optic frequency comb. *Nature* **568**, 378–381 (2019).
22. Zhang M, Buscaino B, Wang C, Shams-Ansari A, Reimer C et al. Broadband electro-optic frequency comb generation in a lithium niobate microring resonator. *Nature* **568**, 373–377 (2019).
23. Barry L P, Del Burgo S, Thomsen B, Watts R T, Reid D A et al. Optimization of optical data transmitters for 40-Gb/s lightwave systems using frequency resolved optical gating. *IEEE Photonics Technol Lett* **14**, 971–973 (2002).
24. Agrawal G P. *Nonlinear Fiber Optics* 3rd ed (Academic Press, San Diego, 2001).
25. Huang Y L, Li Q, Han J Y, Jia Z X, Yu Y S et al. Temporal soliton and optical frequency comb generation in a Brillouin laser cavity. *Optica* **6**, 1491–1497 (2019).
26. Weng H Z, Han J Y, Li Q, Yang Y D, Xiao J L et al. Optical frequency comb generation based on the dual-mode square microlaser and a nonlinear fiber loop. *Appl Phys B* **124**, 91 (2018).
27. Marin-Palomo P, Kemal J N, Karpov M, Kordts A, Pfeifle J et al. Microresonator-based solitons for massively parallel coherent optical communications. *Nature* **546**, 274–279 (2017).
28. Chen Z G, Taylor A J, Efimov A. Coherent mid-infrared broadband continuum generation in non-uniform ZBLAN fiber taper. *Opt Express* **17**, 5852–5860 (2009).
29. Yao C C, Jia Z X, Li Z R, Jia S J, Zhao Z P et al. High-power mid-infrared supercontinuum laser source using fluorotellurite fiber. *Optica* **5**, 1264–1270 (2018).
30. Yao C C, Zhao Z P, Jia Z X, Li Q, Hu M L et al. Mid-infrared dispersive waves generation in a birefringent fluorotellurite microstructured fiber. *Appl Phys Lett* **109**, 101102 (2016).
31. Jia Z X, Yao C C, Jia S J, Wang F, Wang S B et al. 4.5 W supercontinuum generation from 1017 to 3438 nm in an all-solid fluorotellurite fiber. *Appl Phys Lett* **110**, 261106 (2017).

Acknowledgements

We are grateful for financial supports from the National Natural Science Foundation of China (Grant No. 61527823) and the National Key R&D Program of China (Grant No. 2017YFB0405301).

Author contributions

Junyuan Han and Yali Huang contributed equally to this work. All authors commented on the manuscript.

Competing interests

The authors declare no competing financial interests.

Supplementary information

Supplementary information for this paper is available at https://doi.org/10.29026/oea.2020.190033